Stability theory of flat band solitons in nonlinear wave systems

Cheng Shi

Department of Applied Physics and Applied Mathematics,
Columbia University, New York, NY, 10027 USA

Ross Parker

IDA Center for Communications Research, Princeton, Princeton, NJ, 08540, USA

Panayotis G. Kevrekidis

Department of Mathematics and Statistics, University of Massachusetts Amherst, Amherst, 01003-4515, MA, USA
Department of Physics, University of Massachusetts Amherst, Amherst, 01003, MA, USA and
Theoretical Sciences Visiting Program, Okinawa Institute of Science
and Technology Graduate University, Onna, 904-0495, Japan

Michael I. Weinstein

Department of Applied Physics and Applied Mathematics,
Columbia University, New York, NY, 10027, USA and
Department of Mathematics, Columbia University, New York, NY, 10027 USA

(Dated: November 11, 2025)

We establish a sharp criterion for the stability of a class of compactly supported, homogeneous density "minimal compact solitons" or MCS states, of the time-dependent discrete nonlinear Schrödinger equation on a multi-lattice, $\mathbb{L}$ ($\mathbb{L}$-DNLS). MCS states arise for multi-lattices where a nearest neighbor Laplace-type operator on $\mathbb{L}$ has a flat band. Our stability criterion is in terms of the explicit form of the nonlinearity and the projection of distinguished vectors onto the flat band eigenspace. We apply our general results to MCS states of DNLS for the diamond, Kagomé and checkerboard lattices. In lattices where MCS states are unstable, we demonstrate how to engineer the nonlinearity to stabilize small amplitude MCS states. Finally, via systematic numerical computations, we put our analytical results in the context of global bifurcation diagrams.

Introduction: There is significant interest in the dynamics of waves in naturally occurring and engineered crystalline media which exhibit a flat or nearly flat band in their band structure. A consequence of such spectra is the existence of localized, non-transporting and non-dispersing wavepackets or quasi-particles, a property which is used to enhance electron-electron or light-matter interactions in condensed matter [1–5], nonlinear effects in optics and photonics [6–18] and metamaterial systems [19–22]. Among others, some of the experimental platforms in which these phenomena are investigated are: laser-written optical waveguides, e.g., in [11, 12, 14], ultracold atomic systems in periodic lattices [23, 24] or coupled electrical circuits, e.g., in [22, 25].

It is therefore particularly relevant to study the types of stable or long-lived localized excitations that can be supported in nonlinear wave models, whose underlying linear spectrum has a flat band. A prototypical example arises in the discrete nonlinear Schrödinger (DNLS) type wave systems arising in optics, superfluids and materials (see e.g. [26–30]), on the Kagomé lattice [31]. Numerical studies reveal compactly supported nonlinear bound states from which one observes symmetry-breaking bifurcations [32]. While there is substantial analytical theory of solitary wave ("soliton") stability, most information about nonlinear dynamics of coherent structures in systems with linear flat band spectrum has been obtained by direct simulation. A general, unifying theory of the

dynamical stability of the nonlinear states of such systems, is of potential broad interest and our goal in this Letter is to present such a theory.

More specifically, we develop a stability theory of symmetric "minimal" compactly supported homogeneous-density solitons, or simply "minimal compact solitons" (MCS states), of the discrete nonlinear Schrödinger equation on a multi-lattice $\mathbb{L}$ ($\mathbb{L}-$DNLS). Our lattice $\mathbb{L}$ is translation invariant and such that the nearest neighbor Laplacian type operator, $-\Delta_{\mathbb{L}}$, has a flat band at the maximum energy in its spectrum. Examples include the diamond, Kagomé and checkerboard lattices (Figure 1).

Our main result is a general sharp criterion for dynamical stability of minimal compact solitons. We explore the implications of this criterion in the context of the above three multi-lattice examples. For power-law nonlinearities, parametrized by a parameter σ, the bifurcation and stability properties of MCS states are described by two classes of bifurcation diagrams: (a) those for which MCS states are stable for powers, $\mathcal{N} < \mathcal{N}_\star(\sigma)$, a strictly positive threshold, followed by the bifurcation of a symmetry broken branch for $\mathcal{N} > \mathcal{N}_\star(\sigma)$ which destabilizes the MCS, and (b) those for which the MCS states are unstable at any power. In the latter case, our general theory explains how to engineer the nonlinearity in order to stabilize MCS states at small amplitudes. Via detailed numerical bifurcation computations, we put our analytical results in the context of global bifurcation diagrams.

At the heart of our analysis is the observation that, for compactly supported states, the stability/instability analysis reduces to the spectral analysis of a linearized operator; in particular, the point spectrum or eigenvalues of a finite rank perturbation of a discrete "bulk" linear Hamiltonian with a flat band. Using the underlying discrete symmetries of the lattice and the subgroup of symmetries of the MCS states, we reduce this high-dimensional spectral problem to a family of spectral problems for rank one perturbations of the bulk operator acting in orthogonal symmetry subspaces. Strategies of this type have been employed to study symmetry induced band degeneracies; see e.g. [33–35]. In particular, the relevant spectral problems are studied via asymptotic analysis of the resolvent (Green's function) of the linearized operator for large spectral parameter and for the spectral parameter approaching the flat band energy. **Laplacian on a multi-lattice, $\mathbb{L}$ and Flat bands:** Fix a Bravais lattice, $\Lambda \subset \mathbb{R}_x^d$, its dual lattice $\Lambda^* \subset \mathbb{R}_k^d$ and Brillouin zone $\mathcal{B} \subset \mathbb{R}_k^d$. A multi-lattice, $\mathbb{L}$, is a finite union of $N \geq 1$ of translated copies of Λ. The lattice $\mathbb{L}$ can be viewed as the union of $N-$atom cells. A *wave function* is a complex-valued function φ defined on $\mathbb{L}$. Our Hilbert space is $l^2(\mathbb{L})$, the space of complex-valued and square summable wave functions with its usual inner product and norm. We consider the Laplace-type periodic operators $\Delta_{\mathbb{L}}$ on $\mathbb{L}$:

$$\Delta_{\mathbb{L}}\varphi(x) = \sum_{y \sim x} w_{yx}(x)(\varphi(y) - \varphi(x)), \quad x \in \mathbb{L}, \qquad (1)$$

where $\sum_{y \sim x}$ denotes a summation over all $y \in \mathbb{L}$ that are nearest neighbors of x. The connectivity matrix $(w_{xy})_{x,y \in \mathbb{L}}$ is taken to be real and symmetric, and $(x, y) \mapsto w_{xy}$ is $\Lambda \times \Lambda$-periodic. The operator $-\Delta_{\mathbb{L}}$ is bounded, non-negative and self-adjoint on $l^2(\mathbb{L})$. Its band structure is given by the eigenpairs of $N-$ Floquet-Bloch eigenvalue maps: $E_1(k) \leq E_2(k) \leq \cdots \leq E_N(k)$, periodic with respect to Λ^*, with fundamental cell $\mathcal{B}$. Figure 1 displays 3 multi-lattices with their band structures: the diamond lattice $\mathbb{D}$, the Kagomé lattice $\mathbb{K}$, and the checkerboard lattice $\mathbb{C}h$.

The band structure contains a *flat band* if for some $j_0 \in \{1, \ldots, N\}$, $E_{j_0}(k) = E_F$ is a constant for all $k \in \mathcal{B}$. In this paper, we focus on the setting where $-\Delta_{\mathbb{L}}$ has a single flat band at the upper limit, E_F, of its spectrum. The general properties of linear operators with flat bands have been studied extensively. For example, the spectral subspace of $-\Delta_{\mathbb{L}}$ with energy E_F ("flat band eigenspace") contains compactly supported states, and any flat band eigenstate can be approximated by such compactly supported states [36].

Among these compactly supported states is a family of homogeneous density, alternating sign, compact states. This property can be used to obtain lattices with flat-bands via a line graph construction [37–39].

We are interested in *symmetric, minimal and homogeneous alternating compactly supported flat band states* or simply *minimal compact flat band states*. These are func-

tions ψ in the (maximal energy) flat band eigenspace of $-\Delta_{\mathbb{L}}$ such that the following two properties hold:

1. There is a symmetry $\mathfrak{S}: \mathbb{L} \to \mathbb{L}$, cyclic of *even* order s, and a point $x_0 \in \mathbb{L}$ such that $\text{supp}(\psi)$ consists of the s distinct points: $x_0, \mathfrak{S}x_0, \ldots, \mathfrak{S}^{s-1}x_0$. We call this set the orbit of x_0, $\text{Orb}_{\mathfrak{S}}(x_0)$, under the symmetry $\mathfrak{S}$.

2. ψ has uniform amplitude along its support, and $\psi(x) = a \sum_{j=0}^{s-1} (-1)^j \delta_{\mathfrak{S}^j x_0}(x)$ for some $a \neq 0$, and $\delta_y(x)$ denotes the Kronecker delta function at y.
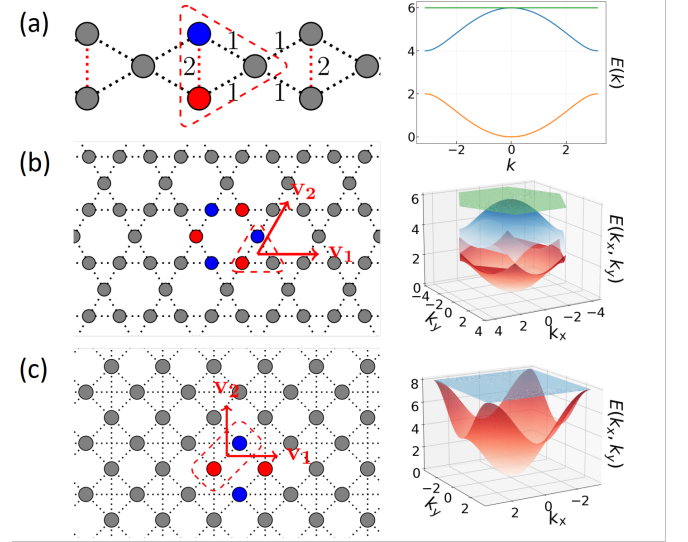

FIG. 1. Lattices, $\mathbb{L}$, and band dispersion loci of $-\Delta_{\mathbb{L}}$ for three cases: (a) Diamond lattice ($\mathbb{L} = \mathbb{D}$) ; (b) Kagomé lattice ($\mathbb{L} = \mathbb{K}$); (c) Checkerboard lattice. ($\mathbb{L} = \mathbb{C}h$). Vertices ("atoms") comprising a fundamental cell are encircled by a dashed curve. Dotted lines connect nearest neighbors. Non-zero connectivity matrix elements, w_{xy}, are labeled for the lattice $\mathbb{D}$. For the lattices $\mathbb{K}$ and $\mathbb{C}h$, $w_{xy} \equiv 1$. The flat band energy occurs at maximum energy of the spectrum of $-\Delta_{\mathbb{L}}$, $E = E_F$; for $\mathbb{D}$ and $\mathbb{K}$, $E_F = 6$, and for $\mathbb{C}h$, $E_F = 8$. Vertices in the support of a minimal compact flat band eigenstate of energy, E_F, are colored red and blue, which denote equal and opposite values of the wavefunction.

The colored vertices in each lattice of Figure 1 mark the support of minimal compact flat band states for the diamond lattice ($d = 1$, $N = 3$; $\mathfrak{S}_{\mathbb{D}} =$ horizontal reflection, $s = 2$; $\psi =$ dipole), the Kagomé ($d = 2$, $N = 3$; $\mathfrak{S}_{\mathbb{K}}$ is $\pi/6$-rotation, $s = 6$; $\psi =$ hexagonal) and the checkerboard lattice ($d = 2$, $N = 2$; $\mathfrak{S}_{\mathbb{C}h}$ is $\pi/4$-rotation, $s = 4$; $\psi =$ square). Any $\Lambda-$translate of these states is also a minimal compact flat band state and the set of all its lattice translates is a dense subset of the l^2- nullspace of $-\Delta_{\mathbb{L}} - E_F$ [40]. **Discrete nonlinear Schrödinger equation:** We consider the discrete nonlinear Schrodinger equation (DNLS) [27] on the lattice $\mathbb{L}$ governing $\Psi \in l^2(\mathbb{L}; \mathbb{C})$:

$$i\partial_t \Psi(x, t) = -\Delta_{\mathbb{L}}\Psi(x, t) + f(|\Psi(x, t)|^2)\Psi(x, t), \qquad (2)$$

$\mathbb{L}$−DNLS is a Hamiltonian system, $i\partial_t \Psi = \delta\mathcal{H}/\delta\overline{\Psi}$. The time-invariant Hamiltonian is given by:

$$\mathcal{H}[\Psi, \overline{\Psi}] := \langle -\Delta_{\mathbb{L}}\Psi(\cdot, t), \Psi(\cdot, t)\rangle_{l^2(\mathbb{L})} + \sum_{x \in \mathbb{L}} F(|\Psi(x,t)|^2), \tag{3}$$

where $F(y) = \int_0^y f(z)\, dz$, and the squared l^2-norm, also known as the *power* of the state Ψ is:

$$\mathcal{N}[\Psi] := \sum_{x \in \mathbb{L}} |\Psi(x,t)|^2. \tag{4}$$

A standing wave solution is of the form $e^{-iE_{\mathrm{nl}}t}\psi(x)$, where $-\Delta_{\mathbb{L}}\psi + f(|\psi|^2)\psi = E_{\mathrm{nl}}\psi$ and $\psi \in l^2(\mathbb{L})$.

Since the nonlinear term in (2) is onsite, any minimal compact flat band state, arising from the flat band of $-\Delta_{\mathbb{L}}$, extends to a nonlinear bound state, a "minimal compact soliton" or MCS state, of $\mathbb{L}$-DNLS (2):

$$\psi_a e^{-iE_{\mathrm{nl}}t} = a \sum_{j=1}^{s} (-1)^j \delta_{\mathfrak{S}^j x_0}(x)\, e^{-iE_{\mathrm{nl}}t}, \tag{5}$$

where $E_{\mathrm{nl}} = E_{\mathrm{nl}}(a) = E_F + f(a^2)$ is an amplitude-dependent nonlinear frequency, and by (5) we have

$$-\Delta_{\mathbb{L}}\psi_a + f(a^2)\psi_a = E_{\mathrm{nl}}\psi_a, \quad \psi \in l^2(\mathbb{L}). \tag{6}$$

In this article we consider *defocusing* or *repulsive* non-linearities of power law type: $f(|x|^2) = |x|^{2\sigma}$, $F(|x|^2) = |x|^{2\sigma+2}/(\sigma + 1)$ [27, 41]. For defocusing nonlinearities, the bifurcation of compactly supported nonlinear bound states is toward frequencies above the linear flat band spectrum, $E_{\mathrm{nl}}(a) > E_F$. Our main result, Theorem 1, characterizes when the minimal compact solitons are dynamically stable and when they are unstable. A universal character of the bifurcation diagram emerges.

Theorem 1. *Assume $-\Delta_{\mathbb{L}}$ has a flat band at the maximum of its spectrum. Consider $\mathbb{L}$-DNLS with power-law defocusing nonlinearity $f(|x|^2) = |x|^{2\sigma}$. Let $\nu \mapsto \psi^\nu$ denote a family of minimal compact solitons, parametrized by $\mathcal{N}[\psi^\nu] = \nu$.*

There exists a critical value of the nonlinearity parameter $0 < \sigma_{\mathbb{L}}^{\mathrm{cr}} \leq \infty$, such that:

(1) for every $\sigma \in (0, \sigma_{\mathbb{L}}^{\mathrm{cr}})$, there is a threshold power $\mathcal{N}_{\mathrm{thr}}(\sigma)$, with $0 < \mathcal{N}_{\mathrm{thr}}(\sigma) < \infty$, such that:
(i) ψ^ν is dynamically stable if $\nu < \mathcal{N}_{\mathrm{thr}}(\sigma)$, and
(ii) ψ^ν is unstable if $\nu > \mathcal{N}_{\mathrm{thr}}(\sigma)$.

(2) for every $\sigma > \sigma_{\mathbb{L}}^{\mathrm{cr}}$, ψ^ν is dynamically unstable for every $\nu > 0$.

The stability / instability transitions corresponding to (i) and (ii) are represented in the schematic of Figure 2.

An extension of the current theory to general nonlinearities, f, will be presented in a forthcoming article [40].

We next discuss the notions of stability and instability in Theorem 1, and the ideas underlying the proof.
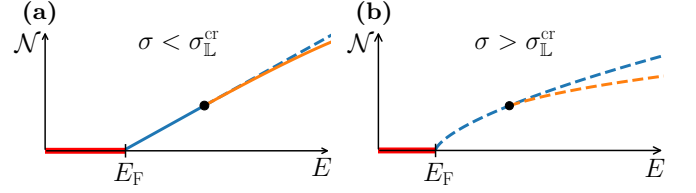

FIG. 2. Universal character of stability transitions for minimal compact solitons (MCS states), which bifurcate from a flat band at $E = E_F$. Theorem 1 implies two possible scenarios: (a) when $\sigma < \sigma_{\mathbb{L}}^{\mathrm{cr}}$, the compact state is at first stable and then transfers its stability to a second branch in a symmetry breaking bifurcation, and (b) when $\sigma > \sigma_{\mathbb{L}}^{\mathrm{cr}}$, the compact state is always unstable. In general, the bifurcation can be sub- or super-critical.

Stability and instability: Our treatment of stability and instability draws inspiration from studies of the stability of ground state solitary waves of the focusing nonlinear Schrödinger equation, e.g. [42–46]. Consider a homogeneous and compactly supported nonlinear bound state, ψ^ν. The set of all phase translations of ψ^ν is the *orbit of ψ^ν*: $\mathcal{O}_{\psi^\nu} := \{\psi^\nu e^{i\theta} : \theta \in [0, 2\pi)\}$. The appropriate notion of stability is *nonlinear orbital stability*; ψ is orbitally stable if $\mathrm{dist}(\Psi(\cdot, t = 0), \mathcal{O}_\psi)$ small implies that $\mathrm{dist}(\Psi(\cdot, t), \mathcal{O}_\psi)$ is small for every $t \neq 0$. Here, $\mathrm{dist}(\Psi(\cdot, t), \mathcal{O}_{\psi^\nu})$ is the minimal l^2-distance from the point $\psi(\cdot, t)$ to the set $\mathcal{O}_{\psi^\nu}$.

The general strategy for determining the orbital stability or instability of a nonlinear bound state is outlined in the End Matter. The analysis reduces to the spectral properties of two linear operators, L_+ and L_-, which arise in the linearized DNLS evolution governing small perturbations. In the case of MCS states, orbital stability is equivalent to the existence of exactly one non-negative eigenvalue in L_+.

Stability/instablity of minimal compact solitons: In the case of power nonlinearities, if ψ_a is an MCS state of amplitude a (see (5)), then $f(|\psi_a|^2) = |a|^{2\sigma}\delta_{\mathrm{supp}(\psi_a)}$, where the subscript denotes the support of the wavefunction ψ_a. The operators $L_\pm$ are then:

$$L_+ = -\Delta_{\mathbb{L}} - E_{\mathrm{nl}}(a) + (2\sigma + 1)|a|^{2\sigma}\delta_{\mathrm{supp}(\psi)} \tag{7a}$$

$$L_- = -\Delta_{\mathbb{L}} - E_{\mathrm{nl}}(a) + |a|^{2\sigma}\delta_{\mathrm{supp}(\psi)}, \tag{7b}$$

where $E_{\mathrm{nl}}(a)$ is displayed just after (5). We next discuss the spectra of L_- and L_+.

First, L_-, as an operator on $l^2(\mathbb{L})$, is negative semi-definite with 0 as its maximum eigenvalue. Indeed, both $-\Delta_{\mathbb{L}} - E_F$ and $|a|^{2\sigma}\delta_{\mathrm{supp}(\psi)} - |a|^{2\sigma}$ are negative semi-definite, and, by (6), $L_-\psi_a = 0$. On the other hand, L_+, as an operator on $l^2(\mathbb{L})$, is indefinite. In fact, by (6), L_+ has a strictly positive eigenvalue: $L_+\psi_a = 2\sigma|a|^{2\sigma}\psi_a$.

In view of the above spectral criterion on L_+, our strategy for assessing the stability or instability of ψ_a is to, for a fixed nonlinearity parameter σ, study the number of positive eigenvalues of L_+, $n_+(a; \sigma)$, as the amplitude parameter a varies; when $n_+(a; \sigma) > 1$, the state ψ_a is unstable. Further, if $n_+(a; \sigma) = 1$, then the above varia-

tional considerations imply nonlinear orbital stability.

Analysis of L_+ as a varies: Since ψ_a is supported on exactly s sites of $\mathbb{L}$, the operator L_+ is a perturbation of the bulk operator $-\Delta_\mathbb{L} - E_{\mathrm{nl}}$ of finite rank equal to s. By the min-max principle of self-adjoint operators, the spectrum of L_+ has at most s eigenvalues above $E_F - E_{\mathrm{nl}}(a) = -|a|^{2\sigma} < 0$, the upper limit of its continuous spectrum. As noted above, L_+ has a strictly positive eigenvalue and hence, for the state ψ_a to be stable, it is necessary that the remaining $\leq s-1$ eigenvalues of L_+ are strictly smaller than zero.

Studying the eigenvalues of L_+ which cross zero energy as a varies, via perturbation theory about the bulk operator:

$$L_{\mathrm{bulk},a} = -\Delta_\mathbb{L} - E_{\mathrm{nl}}(a) = -\Delta_\mathbb{L} - E_F - |a|^{2\sigma}. \quad (8)$$

is subtle since, as $a \to 0^+$, $E_{\mathrm{nl}}(a) \to E_F$, an eigenvalue of infinite multiplicity of $-\Delta_\mathbb{L}$.

Linear algebra and symmetry: Point spectra (eigenvalues) of L_+ are poles of the resolvent operator $\lambda \mapsto (L_+ - \lambda I)^{-1}$ on the real axis and outside the continuous spectrum of L_+. At the core of our analysis lies the fact that the determination of the point spectrum can be reduced, via the Sherman-Morrison-Woodbury identity [47], to an analysis of the zeros of the determinant of an s-by-s matrix, depending analytically on λ and on the amplitude a. A detailed analysis is possible by taking advantage of the symmetries of the lattice $\mathbb{L}$ and of our MCS states.

Let $U_\mathfrak{S}$ be the symmetry on $l^2(\mathbb{L})$ induced by $\mathfrak{S}$: $U_\mathfrak{S} f(x) = f(\mathfrak{S}^{-1}x)$. Since $U_\mathfrak{S}$ is a symmetry of order equal to s, we have $U_\mathfrak{S}^s = \mathrm{Id}$, and thus its eigenvalues are the s-roots of unity $\{\omega^n\}_{n=0}^{s-1}$, where $\omega = e^{2\pi i/s}$. Further, $U_\mathfrak{S}$ is a normal operator, so we may decompose our Hilbert space $l^2(\mathbb{L})$ into an orthogonal sum of s invariant eigenspaces, $l^2_{\omega^n}(\mathbb{L})$, of $U_\mathfrak{S}$: $l^2(\mathbb{L}) = \bigoplus_{n=0}^{s-1} l^2_{\omega^n}(\mathbb{L})$. Second, observe that $U_\mathfrak{S}$ commutes with $-\Delta_\mathbb{L}$ and multiplication by $|a|^{2\sigma}\delta_{\mathrm{supp}(\psi_a)}$, and so $U_\mathfrak{S}$ commutes with L_+. The action of L_+ on $l^2(\mathbb{L})$ can therefore be decomposed into those of s-independent operators L_{+,ω^n}, each defined as L_+ restricted to $l^2_{\omega^n}(\mathbb{L})$. Note that the minimality property of the MCS state ψ_a implies that s, the order of the symmetry, is equal to the rank of the perturbation $L_+ - L_{\mathrm{bulk},a}$.

Next, we represent $\delta_{\mathrm{supp}(\psi_a)} = \sum_{n=0}^{s-1} e_n\langle e_n, \cdot\rangle$, where $e_n \in l^2_{\omega^n}(\mathbb{L})$, $\mathrm{supp}(e_n) = \mathrm{supp}(\psi_a)$, for $n = 0, 1, \ldots, s-1$, and the set $\{e_n\}_{n=0}^{s-1}$ to be an orthonormal subset of $l^2(\mathbb{L})$. Thus, $\delta_{\mathrm{supp}(\psi)}|_{l^2_{\omega^n}(\mathbb{L})} = e_n\langle e_n, \cdot\rangle$ is a rank-one operator $l^2_{\omega^n}(\mathbb{L})$; see the End Matter for further discussion. Therefore, for each $n = 0, \ldots, s-1$,

$$L_{+,\omega^n} = -\Delta_\mathbb{L} - E_{\mathrm{nl}}(a) + (2\sigma+1)|a|^{2\sigma}e_n\langle e_n, \cdot\rangle, \quad (9)$$

a rank one perturbation of $L_{\mathrm{bulk},a}$ on $l^2_{\omega^n}(\mathbb{L})$, given in (8). Moreover, since $-\Delta_\mathbb{L} - E_F$ is negative semi-definite, each L_{+,ω^n} has at most one eigenvalue, denoted $\lambda_n(|a|^{2\sigma})$, above energy $-|a|^{2\sigma}$, the upper edge of the continuous

spectrum of L_{+,ω^n}. Note that, reflecting its oscillatory nature, ψ_a itself lies in the subspace $l^1_{-1}(\mathbb{L})$, i.e., $n = s/2$, and is an eigenstate of $L_{+,-1}$, with eigenvalue $2\sigma|a|^{2\sigma}$.

At this point, we have reduced the problem of determining the point spectrum of L_+ to tracking the $s-1$ simple eigenvalues of the family of operators $\{L_{+,\omega^n}\}_{n\neq s/2}$ as the MCS amplitude varies. Using the Sherman-Morrison-Woodbury identity [47] we can represent the resolvent of L_{+,ω^n} as a perturbation of the resolvent of $L_{\mathrm{bulk},a}$; see the End Matter. For each $n = 0, \cdots, s-1$, the eigenvalue of L_{+,ω^n}, being pole of its resolvent, is given by the zero, $\lambda_n(|a|^{2\sigma})$, of the scalar function:

$$F_n(\lambda, |a|^{2\sigma}) := 1 + (2\sigma+1)|a|^{2\sigma}\langle e_n, R_{\mathrm{bulk},a}(\lambda)e_n\rangle, \quad (10)$$

where $R_{\mathrm{bulk},a}(\lambda) = (L_{\mathrm{bulk},a} - \lambda)^{-1}$. We study $\lambda_n(|a|^{2\sigma})$ as a varies. An asymptotic analysis of $F_n(\lambda, |a|^{2\sigma})$, for $|a|^{2\sigma} \to \infty$ and $|a|^{2\sigma} \downarrow 0$, detailed in the End Matter, yields the sharp stability criterion:

$$\max_{n\neq s/2} \|P_{E_F}^{-\Delta_\mathbb{L}}e_n\|_2^2 < \frac{1}{2\sigma+1}, \quad (11)$$

where $P_{E_F}^{-\Delta_\mathbb{L}}$ denotes the $-\Delta_\mathbb{L}$-spectral projection operator onto the flat band at energy E_F.

If condition (11) is satisfied, then there exists $a_\star > 0$ such that for $0 < a < a_\star$, the $s-1$ eigenvalues $\lambda_n(|a|^{2\sigma})$, with $n \neq s/2$, are strictly negative, and the MCS state of this amplitude is stable. On the other hand, if $a > a_\star$, then at least one of $\lambda_n(|a|^{2\sigma})$ with $n \neq s/2$ becomes positive and we have instability due to the existence of more than one positive eigenvalue of L_+. A typical plot of the motion of $\lambda_n(|a|^{2\sigma})$ under the scenario of condition (11) is given in Figure 3.

If the condition (11) is violated, then for every a, there is at least one $n \neq s/2$ such that $\lambda_n(|a|^{2\sigma}) > 0$, implying a second positive eigenvalue of L_+ along with $2\sigma|a|^{2\sigma}$. In conclusion: *there is a range of amplitudes, $0 < a < a_\star(\sigma)$, of MCS (with corresponding power range, $0 < \mathcal{N} < \mathcal{N}_{thr}(\sigma)$) which are orbitally stable if and only if the spectral condition (11) holds.*

Suppose condition (11) is satisfied. As the amplitude increases, each $\lambda_n(|a|^{2\sigma})$ ($n \neq s/2$) will eventually cross zero. The MCS state ψ_a loses its stability at the first such zero-crossing; see panel (a) of Figure 2. Coincident with each successive crossing, is a new symmetry-broken state which bifurcates from the branch $(\psi_a, E_{\mathrm{nl}}(a))$; see the End Matter discussion of global bifurcations.

To conclude the discussion of Theorem 1, we argue that for generic lattices there is always a $\sigma_\mathbb{L}^{\mathrm{cr}} > 0$. In all examples known to us, and generically we expect: $0 \leq \|P_{E_F}^{-\Delta_\mathbb{L}}e_n\|_2^2 < 1$, i.e., e_n is not a flat-band eigenstate, for every $n \neq s/2$. This condition is independent of the nonlinearity parameter σ. Hence, for small enough $\sigma > 0$, (11) is always guaranteed to be satisfied, therefore establishing the existence of $\sigma_\mathbb{L}^{\mathrm{cr}} > 0$.

Application $\mathbb{D}$, $\mathbb{K}$ and $\mathbb{C}h$ lattices: We now discuss the implications of Theorem 1 for the $\mathbb{D}$, $\mathbb{K}$ and $\mathbb{C}h$ lattices. Recall that our defocusing nonlinearity is $|\psi|^{2\sigma}\psi$. Theorem 1 ensures that if $\sigma < \sigma_\mathbb{L}^{\mathrm{cr}}$ then all sufficiently small
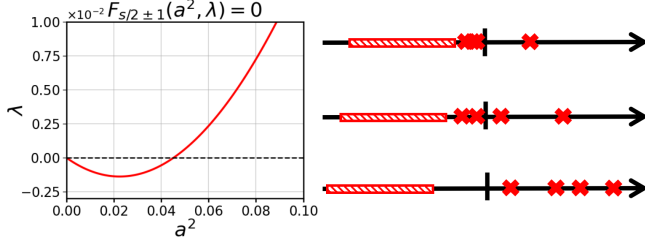
FIG. 3. Motion of eigenvalues, $\lambda_n(|a|^2)$, Kagomé case. Right: Schematic showing $|a|$ small ($\mathcal{N}[\psi_a]$ small), $L_+ = \bigoplus_{n \neq s/2} L_{+,\omega^n}$ has $s-1$ strictly negative eigenvalues in the interval $(-|a|^{2\sigma}, 0)$. As a increases, the discrete eigenvalue of each L_{+,ω^n}, zero of $\lambda \mapsto F_n(\lambda, |a|^{2\sigma})$, crosses zero energy from negative to positive values, and (may) induce successive bifurcations. The minimal compact soliton ψ_a becomes unstable at the first such crossing. Left: Trajectory of $\lambda_{\frac{s}{2}\pm 1}(|a|^2)$ of L_+ as $a > 0$ varies for cubic nonlinearity $\sigma = 1$.

amplitude MCS states are stable (Figure 2, left panel) and if $\sigma > \sigma_{\mathbb{L}}^{\text{cr}}$ all MCS states are unstable (Figure 2, right panel). For $\mathbb{D}$, $\mathbb{K}$ and $\mathbb{C}h$ lattices, our explicit calculation based on (10) yields that the critical nonlinearity values are: $\sigma_{\mathbb{D}}^{\text{cr}} = \infty$, $\sigma_{\mathbb{K}}^{\text{cr}} \approx 1.268$ and $\sigma_{\mathbb{C}h}^{\text{cr}} \approx 0.829$. Theorem 1 implies for the cubic nonlinearity ($\sigma = 1$) that $\mathbb{D}-$ and $\mathbb{K}-$DNLS states are stable below a strictly positive l^2- threshold ($\nu_{\mathbb{D}}^{\star} \approx 2.61$ and $\nu_{\mathbb{K}}^{\star} \approx 0.19$). In fact, for the diamond lattice there is a transition between stable states, at sufficiently small amplitude, and unstable states above some threshold amplitude for any nonlinearity parameter σ (since $\sigma_{\mathbb{D}}^{\text{cr}} = \infty$). For $\mathbb{K}-$DNLS, when $\sigma > \sigma_{\mathbb{K}}^{\text{cr}} \approx 1.268$, all MCS states are unstable. Consider now $\mathbb{C}h-$DNLS, with $\sigma = 1$. Here, MCS states of arbitrary l^2 norm are unstable. However, for $\sigma < \sigma_{\mathbb{C}h}^{\text{cr}} \approx 0.829$ there is a transition between stable sufficiently small amplitude states and unstable states.

Our analysis provides information about the nature of symmetry breaking bifurcations from the branch of MCS states, regardless of their stability. As the amplitude, a, is increased, successive simple eigenvalues of L_{+,ω^n}, for some $n \neq s/2$ pass through zero energy, inducing a bifurcation. The zero energy eigenspace gives an infinitesimal view of the manner in which each bifurcating branch breaks the symmetries of the MCS branch. Figure 4, based on detailed numerical computations, supports Theorem 1, and also shows a global zoomed out view of the various localized states of $\mathbb{L}$-DNLS for $\mathbb{L} = \mathbb{D}, \mathbb{K}$ and $\mathbb{C}h$.

For further discussion, see the End Matter.

Summary and discussion: We have established a sharp criterion for the stability of MCS states of the time-dependent discrete defocusing nonlinear Schrödinger equation on a multi-lattice $\mathbb{L}$ ($\mathbb{L}$-DNLS), and have demonstrated our results for the diamond, Kagomé and checkerboard lattices. For the class of power nonlinearities, we have shown that by adjusting the nonlinearity parameter to be sufficiently small, we can always stabilize the small amplitude MCS states.

We expect the variational, spectral theoretic and symmetry ideas of this article to play a central role in further studies of these and related lattices. For example, (1) flat bands may appear at energies which are interior to the band spectrum. This occurs, for example, in the Lieb lattice, for which DNLS has MCS states; see also the experimental study of a class of diamond lattices [22]. Are such MCS states unstable due to coupling to radiation modes? (2) Here we considered the defocusing nonlinearity, but a natural next step is to complement such studies with a detailed analysis of the focusing case. (3) Another extension of the current study is to lattices arising as line graphs of an underlying lattice [39]. The present paper covers the Kagomé lattice, which is the line graph of the honeycomb lattice and the Checkerboard lattice, which is the line graph of $\mathbb{Z}^2$. Other examples are the line graph of the triangular lattice or the pyrochlore [48], which is the line graph of the 3D diamond lattice. Extensions to such 3D settings would be of particular interest.

[1] R. Bistritzer and A. MacDonald. Moiré bands in twisted double-layer graphene. *Proc. Nat. Acad. Sci*, 108:12233–12237, 2011.

[2] Dumitru Călugăru, Aaron Chew, Luis Elcoro, Yuanfeng Xu, Nicolas Regnault, Zhi-Da Song, and B. Andrei Bernevig. General Construction and Topological Classification of All Magnetic and Non-Magnetic Flat Bands.

Nature Phys., 18(2):185–189, 2022.

[3] Naoyuki Masumoto, Na Young Kim, Tim Byrnes, Kenichiro Kusudo, Andreas Löffler, Sven Höfling, Alfred Forchel, and Yoshihisa Yamamoto. Exciton–polariton condensates with flat bands in a two-dimensional kagome lattice. *New J. Phys.*, 14(6):065002, 2012.

[4] C. E. Whittaker, E. Cancellieri, P. M. Walker, D. R.

Gulevich, H. Schomerus, D. Vaitiekus, B. Royall, D. M. Whittaker, E. Clarke, I. V. Iorsh, I. A. Shelykh, M. S. Skolnick, and D. N. Krizhanovskii. Exciton polaritons in a two-dimensional lieb lattice with spin-orbit coupling. *Phys. Rev. Lett.*, 120:097401, Mar 2018.

[5] Yeongjun Kim, Sergej Flach, and Alexei Andreanov. Real space decay of flat band projectors from compact localized states. *arXiv preprint arXiv:2510.17258v1*, 2025.

[6] Daniel Leykam, Sergej Flach, Omri Bahat-Treidel, and Anton S. Desyatnikov. Flat band states: Disorder and nonlinearity. *Phys. Rev. B*, 88:224203, December 2013.

[7] Daniel Leykam, Alexander Andreanov, and Sergej Flach. Artificial flat band systems: From lattice models to experiments. *Advances in Physics: X*, 3(1):1473052, 2018.

[8] Rodrigo A. Vicencio Poblete. Photonic flat band dynamics. *Advances in Physics: X*, 6(1):1878057, 2021.

[9] Jun-Won Rhim and Bohm-Jung Yang. Singular flat bands. *Advances in Physics: X*, 6(1):1901606, 2021.

[10] Carlo Danieli, Alexei Andreanov, Daniel Leykam, and Sergej Flach. Flat band fine-tuning and its photonic applications. *Nanophotonics*, 13(21):3925–3944, 2024.

[11] D Guzmán-Silva, C Mejía-Cortés, M A Bandres, M C Rechtsman, S Weimann, S Nolte, M Segev, A Szameit, and R A Vicencio. Experimental observation of bulk and edge transport in photonic Lieb lattices. *New J. Phys.*, 16(6):063061, 2014.

[12] Sebabrata Mukherjee and Robert R. Thomson. Observation of localized flat-band modes in a quasi-one-dimensional photonic rhombic lattice. *Opt. Lett.*, 40(23):5443–5446, December 2015.

[13] Sho Kajiwara, Yoshiro Urade, Yosuke Nakata, Toshihiro Nakanishi, and Masao Kitano. Observation of a nonradiative flat band for spoof surface plasmons in a metallic Lieb lattice. *Phys. Rev. B*, 93:075126, February 2016.

[14] Rodrigo A. Vicencio, Camilo Cantillano, Luis Morales-Inostroza, Bastián Real, Cristian Mejía-Cortés, Steffen Weimann, Alexander Szameit, and Mario I. Molina. Observation of localized states in Lieb photonic lattices. *Phys. Rev. Lett.*, 114:245503, June 2015.

[15] Steffen Weimann, Luis Morales-Inostroza, Bastián Real, Camilo Cantillano, Alexander Szameit, and Rodrigo A. Vicencio. Transport in sawtooth photonic lattices. *Opt. Lett.*, 41(11):2414–2417, June 2016.

[16] Shiqiang Xia, Yi Hu, Daohong Song, Yuanyuan Zong, Liqin Tang, and Zhigang Chen. Demonstration of flat-band image transmission in optically induced lieb photonic lattices. *Opt. Lett.*, 41(7):1435–1438, April 2016.

[17] H.S. Nguyen, F. Dubois, T. Deschamps, S. Cueff, A. Pardon, J.-L. Leclercq, C. Seassal, X. Letartre, and P. Viktorovitch. Symmetry breaking in photonic crystals: On-demand dispersion from flatband to dirac cones. *Phys. Rev. Lett.*, 120:066102, February 2018.

[18] Jina Ma, Jun-Won Rhim, Liqin Tang, Shiqi Xia, Haiping Wang, Xiuyan Zheng, Shiqiang Xia, Daohong Song, Yi Hu, Yigang Li, Bohm-Jung Yang, Daniel Leykam, and Zhigang Chen. Direct observation of flatband loop states arising from nontrivial real-space topology. *Phys. Rev. Lett.*, 124:183901, May 2020.

[19] Daniel Leykam, Alexei Andreanov, and Sergej Flach. Artificial flat band systems: from lattice models to experiments. *Adv. Phys.: X*, 3(1):1473052, 2018.

[20] Haiteng Wang, Weixuan Zhang, Houjun Sun, and Xiang-dong Zhang. Observation of inverse anderson transitions in aharonov-bohm topolectrical circuits. *Physical Review B*, 106(10):104203, 2022.

[21] Xiaoqi Zhou, Weixuan Zhang, Houjun Sun, and Xiang-dong Zhang. Observation of flat-band localization and topological edge states induced by effective strong interactions in electrical circuit networks. *Physical Review B*, 107(3):035152, 2023.

[22] Carys Chase-Mayoral, L. Q. English, Noah Lape, Yeongjun Kim, Sanghoon Lee, Alexei Andreanov, Sergej Flach, and P. G. Kevrekidis. Compact localized states in electric circuit flat-band lattices. *Phys. Rev. B*, 109:075430, Feb 2024.

[23] Oliver Morsch and Markus Oberthaler. Dynamics of bose-einstein condensates in optical lattices. *Rev. Mod. Phys.*, 78:179–215, Feb 2006.

[24] V. A. Brazhnyi and V. V. Konotop. Theory of nonlinear matter waves in optical lattices. *Modern Physics Letters B*, 18(14):627–651, 2004.

[25] Noah Lape, Simon Diubenkov, L. Q. English, P. G. Kevrekidis, Alexei Andreanov, Yeongjun Kim, and Sergej Flach. Realization and characterization of an all-bands-flat electrical lattice, 2025.

[26] Falk Lederer, George I. Stegeman, Demetri N. Christodoulides, Gaetano Assanto, Mordechai Segev, and Yaron Silberberg. Discrete solitons in optics. *Physics Reports*, 463(1–3):1–126, 2008.

[27] Panayotis G. Kevrekidis. *The Discrete Nonlinear Schrödinger Equation: Mathematical Analysis, Numerical Computations and Physical Perspectives*, volume 232 of *Springer Tracts in Modern Physics*. Springer, Berlin, Heidelberg, 2009.

[28] Boris A. Malomed, editor. *Spontaneous Symmetry Breaking, Self-Trapping, and Josephson Oscillations*, volume 1 of *Progress in Optical Science and Photonics*. Springer Berlin Heidelberg, Berlin, Heidelberg, 1st edition, 2013. 339 blackandwhite illustrations; 1 in colour.

[29] Mark J. Ablowitz and Justin T. Cole. Nonlinear optical waveguide lattices: Asymptotic analysis, solitons, and topological insulators. *Physica D: Nonlinear Phenomena*, 440:133440, 2022. Review article.

[30] C. Chong and P. G. Kevrekidis. *Coherent Structures in Granular Crystals: From Experiment and Modelling to Computation and Mathematical Analysis*. Springer, New York, 2018.

[31] K. J. H. Law, Avadh Saxena, P. G. Kevrekidis, and A. R. Bishop. Localized structures in kagome lattices. *Phys. Rev. A*, 79:053818, May 2009.

[32] Rodrigo A. Vicencio and Magnus Johansson. Discrete flat-band solitons in the kagome lattice. *Phys. Rev. A*, 87:061803, Jun 2013.

[33] C. L. Fefferman and M. I. Weinstein. Honeycomb lattice potentials and Dirac points. *Journal of the American Mathematical Society*, 25(4):1169–1220, 2012.

[34] R. T. Keller, J. L. Marzuola, B. Osting, and M. I. Weinstein. Spectral band degeneracies of $\frac{\pi}{2}$-rotationally invariant periodic Schrödinger operators. *Multiscale Modeling & Simulation*, 16(4):1684–1731, 2018.

[35] A. Drouot and C. Lyman. Band spectrum singularities for schrödinger operators. *https://arxiv.org/abs/2410.02092*, 2025.

[36] Peter Kuchment. Quantum graphs ii: Some spectral properties of quantum and combinatorial graphs. *Journal of Physics A: Mathematical and Theoretical*, 38(22):4887–4900, 2005.

[37] Andreas Mielke. Ferromagnetic ground states for the

hubbard model on line graphs. *Journal of Physics A: Mathematical and General*, 24(2):L73–L77, 1991.

[38] Andreas Mielke. Ferromagnetism in the hubbard model on line graphs and further considerations. *Journal of Physics A: Mathematical and General*, 24(14):3311–3321, 1991.

[39] Alicia J. Kollár, Mattias Fitzpatrick, Peter Sarnak, and Andrew A. Houck. Line-graph lattices: Euclidean and non-euclidean flat bands, and implementations in circuit quantum electrodynamics. *Communications in Mathematical Physics*, 376(3):1909–1956, 2020.

[40] C. Shi, R. Parker, P. G. Kevrekidis, and M.I. Weinstein. Flat band lattices and nonlinear bound states in discrete nonlinear wave equations. *in preparation*.

[41] J. Cuevas, P.G. Kevrekidis, D.J. Frantzeskakis, and B.A. Malomed. Discrete solitons in nonlinear schrödinger lattices with a power-law nonlinearity. *Physica D: Nonlinear Phenomena*, 238(1):67–76, 2009.

[42] Michael I. Weinstein. Lyapunov stability of ground states of nonlinear dispersive evolution equations. *Communications on Pure and Applied Mathematics*, 39(1):51–67, 1986.

[43] Manoussos Grillakis, Jalal Shatah, and Walter Strauss. Stability theory of solitary waves in the presence of symmetry, i. *Journal of Functional Analysis*, 74(1):160–197, 1987.

[44] Manoussos G. Grillakis. Linearized instability for nonlinear schrödinger and klein-gordon equations. *Communications on Pure and Applied Mathematics*, 41(6):747–774, 1988.

[45] Michael I. Weinstein. Excitation thresholds for nonlinear localized modes on lattices. *Nonlinearity*, 12(3):673–691, 1999.

[46] Michael I. Weinstein. *Localized states and their dynamics in the nonlinear Schroedinger / Gross-Pitaeveskii equation: Analysis and Applications*, volume 3. Springer, 2015.

[47] G.H. Golub and C.F. Van Loan. *Matrix Computations, 4th ed.* Johns Hopkins, 2013, 2015.

[48] Jianwei Huang, Chandan Setty, Liangzi Deng, Jing-Yang You, Hongxiong Liu, Sen Shao, Ji Seop Oh, Yucheng Guo, Yichen Zhang, Ziqin Yue, Jia-Xin Yin, Makoto Hashimoto, Donghui Lu, Sergey Gorovikov, Pengcheng Dai, Jonathan D. Denlinger, J. W. Allen, M. Zahid Hasan, Yuan-Ping Feng, Robert J. Birgeneau, Youguo Shi, Ching-Wu Chu, Guoqing Chang, Qimiao Si, and Ming Yi. Observation of flat bands and dirac cones in a pyrochlore lattice superconductor. *npj Quantum Materials*, 9, 2024.

[49] C.K.R.T. Jones. Instability of standing waves for nonlinear schrödinger-type equations. *Ergod. Th. & Dynam. sys.*, 8:119–138, 1988.

[50] Michael Reed and Barry Simon. *Methods of Modern Mathematical Physics, Volume IV: Analysis of Operators*. Academic Press, New York, 1978.

End Matter

Framework for stability / instability analysis. A nonlinear standing wave $\psi^\nu e^{-iEt}$ is a critical point in $l^2(\mathbb{L})$ of $\mathcal{H}[u]$ subject to the constraint $\mathcal{N}[u] = \nu$, i.e. for some $E_{\mathrm{nl}} = E_{\mathrm{nl}}(\nu)$, ψ^ν satisfies $\delta\mathcal{E}[\psi^\nu] = 0$, where $\mathcal{E}[u] \equiv \mathcal{H}[u] - E_{\mathrm{nl}}(\nu)\mathcal{N}[u]$. A strategy to explore whether a state ψ^ν is stable is to examine whether ψ^ν is a local constrained maximizer [42, 43, 45]. To this end, we let $\psi \in l^2(\mathbb{L})$ such that $\mathcal{N}[\psi] = \nu$, and choose $\theta_\star$ so that $\|\psi - e^{i\theta_\star}\psi^\nu\| = \mathrm{dist}\big(\psi, \mathcal{O}_{\psi^\nu}\big)$. Writing $u + iv = \psi - e^{i\theta_\star}\psi^\nu$ we have $\mathcal{H}[\psi] - \mathcal{H}[\psi^\nu] \approx \langle L_+ u, u\rangle + \langle L_- v, v\rangle$, where, for the case of MCS states under power law nonlinearities, $L_\pm$ are displayed in (7). The optimality of $\theta_*(t)$ implies $\langle \psi^\nu, v\rangle = 0$, and $\mathcal{N}[\psi] = \mathcal{N}[\psi^\nu]$ implies $\langle \psi^\nu, u\rangle = 0$. As operators on $l^2(\mathbb{L})$, L_- is negative semi-definite and L_+ is indefinite and has at least one positive eigenvalue. Hence, the state ψ^ν is a constrained local maximizer and is (orbitally Lyapunov) stable if the above quadratic form in (u, v), subject to the orthogonality constraint on u, is negative definite. Since the MCS ψ^ν itself is an eigenvector of L_+ with a strictly positive eigenvalue, it follows from the orthogonality constraint that a sufficient condition for ψ^ν being a constrained local maximizer is that all other eigenvalues of L_+ are strictly negative, i.e., L_+ has only one non-negative eigenvalue.

On the other hand, conditions on the spectra of L_+ and L_-, which imply the existence of unstable eigenvalues of the linearized time-evolution, were established in [44, 49] in the context of solitary standing waves of the continuum *focusing* NLS equation. Adapting the results of [44] to MCS states of defocusing $\mathbb{L}-$DNLS, we have that: a sufficient condition for linearized instability (a time exponentially growing linearized solution) is that the number of strictly positive eigenvalues of L_+ is strictly larger than one.

Use of the properties of MCS states in the spectral analysis. The proof of Theorem 1 reduces the spectral analysis of L_+ to the family of rank one operators $\{L_{+,\omega^n}\}_{n=s/2}$; see (9). L_{+,ω^n} is given in terms of $e_n \in l^2_{\omega^n}(\mathbb{L})$ ($n \neq s/2$), which is localized on the support of ψ_a. The states e_n can be characterized using the following observation: since $e_n \in l^2_{\omega^n}(\mathbb{L})$ and $\mathrm{supp}(e_n) = \mathrm{Orb}_{\mathfrak{S}}(x)$ for some $x \in \mathbb{L}$ with $|\mathrm{Orb}_{\mathfrak{S}}(x)| = s$, e_n is generated by $e_n(x)$, because $e_n(\mathfrak{S}x) = \omega^{-n}e_n(x)$. This suggests that each e_n acts as a "wave function" and forms a Fourier-type basis on $\mathrm{supp}(\psi_a)$.

Calculating the resolvent L_{+,ω^n} is tractable via the Sherman-Morrison-Woodbury identity [47], which yields an expression for $(L_{+,\omega^n} - \lambda\mathrm{I})^{-1}$ a rank one perturbation of the resolvent of the bulk operator, which is unbounded only on the continuous spectrum. For each $n \neq s/2$, there is a single pole of the resolvent (point eigenvalue of L_{+,ω^n}) at the zero, $\lambda_n(|a|^{2\sigma})$, of the function $F_n(\lambda, |a|^{2\sigma})$, which is displayed in Eq. (10).

Fix $n \neq s/2$. We study the eigenvalue curves $|a|^{2\sigma} \in (0, \infty) \mapsto \lambda_n(|a|^{2\sigma})$. Note first that $F_n(|a|^{2\sigma}, \lambda = 0) \to -2\sigma < 0$ as $|a|^{2\sigma} \to \infty$. Next, by the functional calculus

of self-adjoint operators [50], we have

$$\lim_{|a|^{2\sigma} \to 0} F_n(|a|^{2\sigma}, \lambda = 0) = 1 - (2\sigma+1)\big\|P_{\{E_F\}}(-\Delta_{\mathbb{L}})e_n\big\|^2.$$

Hence, if $\big\|P_{\{E_F\}}(-\Delta_{\mathbb{L}})e_n\big\|^2 < (2\sigma + 1)^{-1}$, then $F_n(0^+, 0) > 0$. Therefore, by continuity, there exists $a_0(n) > 0$, for which $\lambda_n(|a_0(n)|^{2\sigma}) = 0$. Implicit differentiation shows that $|a|^{2\sigma} \mapsto \lambda_n(|a|^{2\sigma})$ is strictly increasing once $\lambda_n(|a|^{2\sigma}) \geq 0$, which implies the uniqueness of the zero crossing point $a_0(n)$. A detailed and rigorous analysis is carried out in [40].

Therefore, as a increases through $a_0(n)$, the eigenvalue $\lambda_n(|a|^{2\sigma})$ transitions from the interval $-|a|^{2\sigma} < \lambda < 0$ to positive values. It follows that if condition (11) is satisfied then for $0 < a < a_\star := \min_{n \neq s/2} a_0(n)$, the $s - 1$ eigenvalues $\lambda_n(|a|^{2\sigma})$, with $n \neq s/2$, are strictly negative and we have stability of the MCS state ψ_a.

Global study of bifurcations. For the diamond lattice, $\mathbb{D}$, the MCS state is a dipole supported on two sites. It can be proved that $\sigma_{\mathbb{D}}^{\mathrm{cr}} = \infty$. As seen in Fig. 4(a), for $\sigma = 1$, the dipole state is stable for $\mathcal{N} < \nu_\star \approx 2.61$ [branch #1], and becomes unstable for $\mathcal{N} > \nu_\star$, which is consistent with Theorem 1. At $\nu_\star$, L_+, the linearized operator about the dipole, has a nontrivial nullspace, which triggers a bifurcation. The corresponding zero eigenstate exhibits even horizontal reflection symmetry, a symmetry not shared by the anti-symmetric dipole. The resulting bifurcating branch therefore breaks the symmetry type of the MCS state, and emerges as an asymmetric dipole [branch #2]. The states on this new branch are no longer compactly supported. Fig. 4(a) displays additional solutions ("single-site" [branch #3] and "double" [branch #5]) which are not compactly supported and bifurcate from the quadratic band; both are unstable.

For the Kagomé lattice, $\mathbb{K}$, the MCS state interacts with other solution branches via bifurcation when ($\sigma = 1 < 1.268 \approx \sigma_{\mathbb{K}}^{\mathrm{cr}}$); see Fig. 4(b). The MCS hexagonal states [branch #1] are stable at small power. At $\nu_\star$, this stability is lost through a symmetry-breaking bifurcation associated with a nontrivial kernel of L_+. The resulting asymmetric solution [branch #2] eventually connects to the single-site state [branch #3], which is unstable until this bifurcation point. This behavior was numerically reported in [32] and is mathematically explained herein.

A somewhat analogous scenario occurs for the checkerboard lattice, $\mathbb{C}h$, in Fig. 4(d). When $\sigma = 0.6 < \sigma_{\mathbb{C}h}^{\mathrm{cr}} \approx 0.829$, the MCS square state [branch #1] loses stability at a power $\nu_\star$. Similar to the Kagomé lattice, the corresponding zero crossing of an eigenvalue of L_+ induces bifurcation of an intermediate branch #2, which then connects to the single-site state branch #3. In contrast to $\mathbb{K}$, the bifurcation at $E_{\mathrm{nl}} \approx 2.3$ is subcritical; both branches #1 for $\nu > \nu_\star$ and #2 for $\nu < \nu_\star$ are unstable.

Consistent with Theorem 1, we observe instability of all hexagonal MCS states for quartic nonlinearity ($\sigma = 1.5 > \sigma_{\mathbb{K}}^{\mathrm{cr}} \approx 1.268$) in $\mathbb{K}$ (Fig. 4(c)), as well as of all square MCS states for cubic nonlinearity ($\sigma = 1 > \sigma_{\mathbb{C}h}^{\mathrm{cr}} \approx 0.829$) in $\mathbb{C}h$ (Fig. 4(e)).
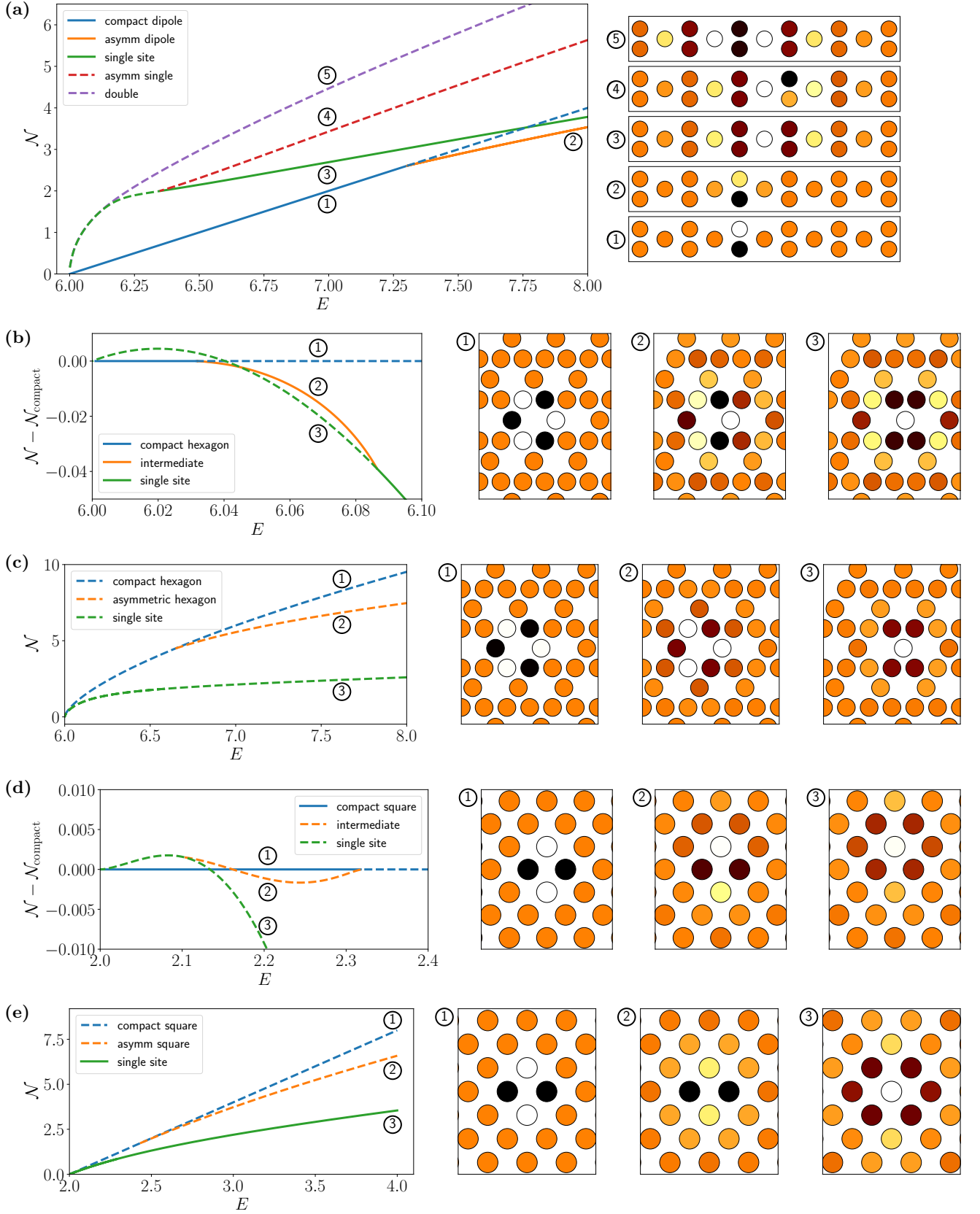
FIG. 4. Bifurcation diagrams plotting power $\mathcal{N}$ vs. nonlinear frequency E for diamond lattice, Kagomé lattice, and checkerboard lattice. (a) Diamond lattice $\mathbb{D}-$DNLS with $\sigma = 1$. (b) and (c), Kagomé lattice $\mathbb{K}-$DNLS with $\sigma = 1 < \sigma_{\mathbb{K}}^{\mathrm{cr}}$, and $\sigma = 1.5 > \sigma_{\mathbb{K}}^{\mathrm{cr}}$, respectively. (d) and (e), Checkerboard lattice $\mathbb{C}h-$DNLS with $\sigma = 0.6 < \sigma_{\mathbb{C}h}^{\mathrm{cr}}$, and $\sigma = 1 > \sigma_{\mathbb{C}h}^{\mathrm{cr}}$, respectively. Solid lines indicate spectral stability, dotted lines indicate spectral instability. (The vertical axis for (b) and (d) is the difference between the power of the solution and the power of the compact solution, which was chosen for ease of visualization).